Title	Plasma Waves Causing Relativistic Electron Precipitation Events at International Space Station: Lessons From Conjunction Observations With Arase Satellite
Authors	Ryuho Kataoka, Yoichi Asaoka, Shoji Torii, Satoshi Nakahira, Haruka Ueno, Shoko Miyake, Yoshizumi Miyoshi, Satoshi Kurita, Masafumi Shoji, Yoshiya Kasahara, Mitsunori Ozaki, Shoya Matsuda, Ayako Matsuoka, Yasumasa Kasaba, Iku Shinohara, Keisuke Hosokawa, Herbert Akihito Uchida, Kiyoka Murase, Yoshimasa Tanaka
Citation	Journal of Geophysical Research: Space Physics, 125(9), 1-11, 2020
Issue Date	2020-8-14
Type	Journal Article
URL	https://doi.org/10.1029/2020JA027875
Right	
Textversion	author

Plasma waves causing relativistic electron precipitation events at International Space Station: Lessons from conjunction observations with Arase satellite

Ryuho Kataoka[1,2], Yoichi Asaoka[3], Shoji Torii[3], Satoshi Nakahira[4], Haruka Ueno[5], Shoko Miyake[6], Yoshizumi Miyoshi[7], Satoshi Kurita[7], Masafumi Shoji[7], Yoshiya Kasahara[8], Mitsunori Ozaki[8], Shoya Matsuda[4], Ayako Matsuoka[4], Yasumasa Kasaba[9], Iku Shinohara[4], Keisuke Hosokawa[10], Herbert Akihito Uchida[2], Kiyoka Murase[2], and Yoshimasa Tanaka[1,2,11]

[1]National Institute of Polar Research, 10-3 Midori-cho, Tachikawa, Tokyo 190-8518, Japan

[2]Department of Polar Science, SOKENDAI, 10-3 Midori-cho, Tachikawa, Tokyo 190-8518, Japan

[3]Waseda Research Institute for Science and Engineering, Waseda University, 3-4-1 Okubo, Shinjuku, Tokyo 169-8555, Japan

[4]Institute of Space and Astronautical Science, Japan Aerospace Exploration Agency, 3-1-1 Yoshinodai, Chuo-ku, Sagamihara, Kanagawa, 252-5210, Japan

[5]Research and Development Directorate, Japan Aerospace Exploration Agency, 2-1-1 Sengen, Tsukuba, Ibaraki 305-8505, Japan

[6]National Institute of Technology (KOSEN), Ibaraki College, 866, Nakane,Hitachinaka-shi,Ibaraki-ken 312-8508 Japan

[7]Institute for Space-Earth Environmental Research, Nagoya University, Furo-cho, Chikusa-ku, Nagoya, Aichi, 464-8601, Japan

[8]Graduate School of Natural Science and Technology, Kanazawa University, Kakumamachi, Kanazawa, Ishikawa, 920-1192, Japan

[9] Planetary Plasma and Atmospheric Research Center (PPARC), Graduate School of Science, Tohoku University, Aramaki-aza-Aoba 6-3, Aoba, Sendai, Miyagi 980-8578, Japan

[10]Department of Communication Engineering and Informatics, The University of Electro-Communications, 1-5-1 Chofugaoka, Chofu, Tokyo, 182-8585, Japan

[11]Joint Support-Center for Data Science Research, 10-3 Midori-cho, Tachikawa, Tokyo, 190-0014, Japan

Corresponding author: first and last name (kataoka.ryuho@nipr.ac.jp)

Key Points:

- Three different types of relativistic electron precipitation (REP) events are observed at International Space Station (ISS).
- Electromagnetic ion cyclotron waves were observed during a REP event at conjugate locations near the magnetic equator.

- Whistler mode waves were observed during other REP events at conjugate locations near the magnetic equator.

Abstract

We report three different types of relativistic electron precipitation (REP) events observed at International Space Station (ISS), associated with electromagnetic ion cyclotron (EMIC) waves or whistler mode waves as observed by the Arase satellite at conjugate locations near the magnetic equator. Three different detectors installed on the ISS were complementarily used; CALET/CHD as the detector of precipitating MeV electrons, MAXI/RBM as the detector of sub-MeV electrons from horizontal and vertical directions, and SEDA-AP/SDOM to quantitatively measure the energy spectrum. The REP event on August 21, 2017 shows a quasi-periodic intensity variation at ~1 Hz which corresponds to variations of the EMIC waves at the Arase altitudes. The REP event on April 24, 2017 shows rapid and irregular intensity variation which corresponds to the amplitude variation of chorus waves, while the REP events on October 26, 2017 shows a smooth quasi-periodic time variation at ~0.2 Hz which corresponds to the amplitude variation of "electrostatic" whistler mode waves. This study clearly demonstrates that the time variation of REP events at ISS are caused by various types of plasma waves near the magnetic equator.

Plain Language Summary

Several different kinds of plasma waves were identified in the magnetosphere as the possible cause of relativistic electron precipitation (REP) events at International Space Station (ISS).

1 Introduction

Relativistic electrons of more than several hundred keV precipitate into the Earth's atmosphere with various spatiotemporal scales. The relativistic electron precipitation (REP) events have been detected by ground-based observations (Bailey and Pomerantz, 1965; Rosenberg et al., 1972), and then observed by balloon and satellite observations (e.g., Anderson et al., 1968; Imhof et al., 1986; Nakamura et al., 1995, 2000; Blake et al., 1996; Lorentzen et al., 2000; Carson et al., 2013; Comess, et al., 2013). The importance of understanding REP events has been increasing since the REP events have been clearly identified at International Space Station (ISS) (Kataoka et al., 2016). Ueno et al. (2019) quantitatively evaluated the exposure dose rate of REP events during extra-vehicle activity at ISS.

Revealing the cause of the REP events contributes to predicting the dynamic variation of the radiation belts, because it is one of the essential components leading to the loss process of the outer belt electrons into the atmosphere (Lorentzen et al. 2000; Millan et al., 2002; Miyoshi et al., 2008, 2015a; Kubota et al. 2015; Kurita et al., 2018). The related ionization of the middle atmosphere and their possible impacts on changing the atmospheric trace components have also been quantitatively evaluated (Daae et al., 2012; Isono et al., 2014a, 2014b; Miyoshi et al., 2015a; Turunen et al., 2016, Kataoka et al., 2019).

The dominant occurrence of REP events at ISS in the pre-midnight sector near the plasmapause is consistent with the hypothesis that the electromagnetic ion cyclotron (EMIC) waves play an important role to cause the REP events at ISS (Kataoka et al., 2016), assuming that EMIC waves are efficiently resonant with MeV electrons (Millan and Thorne, 2007; Miyoshi et al., 2008; Kubota et al., 2015), although whistler mode waves can also be resonant with broad energy range of electrons from tens-keV to MeV electrons as propagating from magnetic equator toward off-equator mainly at the dawn-side magnetosphere (Miyoshi et al., 2015a). The purpose of this paper is to identify the plasma waves which caused the REP events,

from the conjugate observations between the Arase satellite and SEDA-AP (Space Environment Data Acquisition equipment - Attached Payload), CALET (Calorimetric Electron Telescope), and MAXI (Monitor of All-sky X-ray Image) onboard ISS. Section 2 describes the instrumentation. Section 3 describes the method of identifying conjugate events. Section 4 shows the results of multi-event study. The obtained results are discussed in Section 5. Concluding remarks are shown in Section 6.

2 Instrumentations

The Arase satellite started the full in-situ observation of energetic particles and plasma waves from March 2017 (Miyoshi et al. 2018a). The plasma wave data shown in this study are measured by the onboard frequency analyzer (OFA) and Electric Field Detector (EFD) of the plasma wave experiment (PWE) and Magnetic Field Experiment (MGF) onboard the Arase satellite (Kasaba et al., 2017; Kasahara et al. 2018; Matsuda et al. 2018; Matsuoka et al., 2018; Ozaki et al. 2018a).

The best data set from the ISS exposure module is available for approximately two and a half years from October 2015 to March 2018, when three different instruments were operative at the same time as briefly explained below. The SEDA-AP completed its operation in March 2018, while the CALET started its observation in October 2015. The MAXI has continued observation since August 2009. Table 1 shows the energy ranges of each instrument onboard ISS used in this study.

CALET has been carrying out the observations of GeV-TeV electrons, nuclei in Z=1-40, gamma-rays above 1 GeV and gamma-ray bursts since 2015. (Torii et al., 2017; Asaoka et al., 2018). The charge detector (CHD) placed on top of the CALET instrument is consisted of segmented plastic scintillators to measure the electric charge of incident particles. The layers of paddles CHD-X and CHD-Y are orthogonally arranged to determine the incident position of cosmic rays. The trigger counter signals are counted, and the accumulated numbers are recorded every 1 s, which is utilized to monitor the radiation environment. As shown in Kataoka et al. (2016), we are able to use this count rate to study MeV electrons, although CHD-X and CHD-Y are also sensitive to energetic protons above 19 MeV and 47 MeV, respectively. Note that the time cadence of CALET/CHD count rate data can be enhanced by analyzing the recorded counts at each cosmic ray events. In this study we show later 0.1 s averaged values of the event-trigger data.

Radiation belt monitor (RBM) of the MAXI instrument (Matsuoka et al., 2009) has a time resolution of 1 s, and it is sensitive to electrons and protons above 0.3 and 3 MeV, respectively. There are two identical sensors, RBM-H and RBM-Z, directing toward horizontal and vertical (zenith) directions, respectively. RBM-Z sensor is therefore sensitive to energetic electron precipitations.

The SDOM (standard dose monitor) has sensitivities to electron from 0.28 to 20.01 MeV and proton from 1 to 250 MeV (Matsumoto et al., 2001). It can discriminate electrons from protons and the electron trigger counts are accumulated at every 10 s with seven energy channels. However, the highest energy channels, CH6 and CH7 are not used in this paper because it is contaminated with cosmic-ray protons. During the relocation of SEDA-AP in August 2015, the line of sight of the SDOM was changed from the original zenith direction to the current 90 degrees from zenith direction.

Note that the CHD and RBM instruments onboard ISS were not originally designed to measure the energetic electrons but also possibly affected by energetic protons and other energetic particles. Nevertheless, a majority of REP events can be interpreted to be energetic electrons from a statistical comparison among CHD, RBM, and SDOM, as also supported by our previous studies of multi-event analysis (Kataoka et al., 2016) and a statistical analysis (Ueno et al. 2019; and the REP event list therein). The only exception we found so far is a major solar proton events in September 2017, which were excluded from the present study.

3 Event detections

The systematic survey of conjugate REP events was conducted for the whole one-year data from March 2017 to March 2018 when three instruments of ISS (CHD, RBM, SDOM) and the Arase satellite plasma wave data are available. Science data of the Arase satellite were obtained from the ERG Science Center (Miyoshi et al., 2018b), and the SPEDAS data analysis system (Angelopoulos et al., 2019) are used throughout this study. Here we briefly explain the detection procedure of conjunction REP events.

First, we identified the conjunction events between the ionospheric footprints of the Arase satellite and the ISS orbit, where the Arase footprints were calculated by the IGRF model. We allowed the longitudinal difference of 5.0 deg, and the latitudinal difference of 2.5 deg to identify the coarse-cut conjunction events, before using Tsyganenko models. The obtained conjunction event list and the quick-look plots are open to public at our website (http://maxi.riken.jp/nakahira/conjunc_20170822055235_9j23ds484ktmjx9l9/ergiss/).

Second, from the conjunction events, we selected the largest REP events when the CHD-X count rate approached to or exceeded 10^5 Hz. T04s geomagnetic field model (Tsyganenko and Sitnov, 2005) is then used to examine the Arase footprint in detail to further exclude bad conjunction events around the peak time of the CHD-X count rate. In this paper we show the detailed analysis of the three selected REP events in which the complete data set were available.

As shown in Figure 1, the selected events occurred at pre-midnight to midnight sector. The ISS passed across the 55-65 CGMLAT in altitude-adjusted corrected geomagnetic coordinates (Shepherd, 2014), and spanning several hours of magnetic local time (MLT) within a short time interval of 10 min, while the Arase satellite did not largely change the position during the 10 min. These are the best events in terms of the conjunctions between the ISS orbit and the Arase footprint, but still, possible differences between the REP events at ISS (red plus signs) and the Arase footprint (diamonds) is as large as a few degrees in latitudes and 1 MLT in longitude, as shown in Figure 1. The unique trajectories of ISS across such a wide latitude and longitude range in a short time, however, can provide new information of the possible spatial areas which have correlations between the precipitated electrons and plasma waves near the magnetic equator.

Figure 2 shows the high time cadence 0.1 s data of CHD count rate for the identified REP events. A quasi-periodic variation at ~1 Hz was observed during the REP event on August 21, 2017. On the other hand, the CHD count rate shows an irregular change during the REP event on April 24, 2017. The time variation is relatively smooth and quasi-periodic at 0.2 Hz during the REP event on October 26, 2017. In the following section we show our new finding that the three

different time profiles as shown in Figure 2 correspond to three different types of plasma waves excited in the magnetosphere.

4 Results

4.1 EMIC event on August 21, 2017

The details of the REP event on August 21, 2017 is shown in Figure 3, together with the data from Arase satellite. During this REP event, the count rates were high at both CHD-X and CHD-Y (Figure 3c), which indicated the large flux of energetic electrons beyond 3.6 MeV, as also indicated by SDOM data. RBM data shows that sub-MeV electrons were not particularly enhanced during this REP event (Figure 3a), which is consistent with the moderate activity of whistler mode waves as shown in the bottom panels of Figure 3.

As shown in Figure 4, The He+ band EMIC waves of 0.5-1.0 Hz, as well as the proton band at 1.0-2.0 Hz, were clearly observed at 1735-1800 UT when the Arase satellite approached toward magnetic equator at from 20 MLAT to 18 MLAT at ~23 MLT. Assuming that a few min timing difference between the REP event and EMIC waves are due to the spatial structures, these observational facts shown in Figures 3 and 4 are consistent with the hypothesis that the scattering of MeV electrons by EMIC waves caused this REP event at ISS.

However, the He+ band EMIC waves cannot likely cause the precipitating electrons as observed by CHD-X and CHD-Y (Figure 3c) because the resonant energy (e.g., Miyoshi et al., 2008) is estimated to be >4 MeV, and if it works the count rate of CHD-X should be comparable to that of CHD-Y (see Table 1). On the other hand, the resonant energy of proton band EMIC waves is estimated to be a few MeV, which is consistent with the observed electrons, and the possible subpacket structure (e.g., Kubota et al., 2017) can also naturally cause the rapid ~1 Hz modulation in the precipitating electrons as seen in Figure 1a. It is therefore possible that the proton band EMIC waves played an essential role to cause the REP event, although the Arase satellite was likely too far from the magnetic equator to directly observe the strong activity of the proton band. Here we calculated the resonance energy at the magnetic equator, and assumed that the ion densities are the same at the Arase location and at magnetic equator with the ion composition ratio of 70% H+, 20% He+, and 10% O+. Note also that Denton et al. (2019) suggested that the ion composition ratio changes the minimum resonance energy.

The REP event on August 21, 2017 occurred at around the end of the growth phase of a moderate substorm with the peak AE index of ~500 nT when the substorm expansion phase started at 1740 UT and peaked at 1750 UT. The Kp index was only 1+, without magnetic storm activity. The solar wind speed was high at ~560 km/s, as originated from a large coronal hole in the northern hemisphere of the Sun. Note that this event is different from the results from Tanaka et al. (2019), who showed a mesospheric ionization event associated with EMIC waves during a compressed solar wind structure of corotating interaction region. No significant pressure pulses were identified in the solar wind data, and the possible trigger of this REP event and the substorm expansion can be a typical directional discontinuity of the interplanetary magnetic field rotating from southward Bz to northward Bz, and from positive By to negative By.

4.2 Chorus event on April 24, 2017

The REP event on April 24, 2017 occurred during a continuous substorm activity (AE index of ~700 nT) within a recovery phase of a moderate magnetic storm (SYM-H index of ~-30 nT), as also driven by the high-speed solar wind flowing from a large equatorial coronal hole at the Sun. In fact, the solar wind speed was very high at ~650 km/s. The Kp index was also high at 4-.

The Arase satellite was located at around the magnetic midnight, and out of magnetic equator at -23 MLAT. Whistler mode chorus waves were observed in several multiple bands as shown in the bottom panels of Figure 5. There was a data gap of EFD and MGF for this time interval, and we cannot judge whether EMIC waves were observed or not.

The ISS was located at midnight at 1834 UT and peaked at 63 CGMLAT, and passed across the REP zone of 60-63 CGMLAT from 22 MLT to 2 MLT. The electron spectra in the pre-midnight is more energetic (moderately active in RBM count rate), and less energetic (active in RBM count rate) in post-midnight.

ISS was at a few deg higher magnetic latitude than the Arase footprint according to T04s mapping. Nevertheless, as indicated by arrows in Figure 5, the time profile of CHD count rate (>1.6 MeV electrons) shows correlation with the amplitude variation of low-frequency component (<0.1 fce) of whistler mode waves, while RBM-Z count rate (>0.3 MeV electrons) is correlated with that of high-frequency component (>0.1 fce). Such a relationship is consistent with the theoretical expectation of resonant electron scattering by chorus waves propagating toward high magnetic latitude along the magnetic field (Miyoshi et al., 2015a). As a reference, the resonant energies of precipitating electrons for 0.05 fce and 0.5 fce are estimated to be 1-2 MeV and 0.2-0.5 MeV, respectively (Miyoshi et al., 2015a), which are consistent with the observations.

It is therefore suggested that relatively low-frequency whistler-mode chorus waves which propagated away from magnetic equator are the possible origin of this REP event. Considering the trajectory of ISS across the wide latitude and longitude range during the several min time period of high count rates of both CHD-X and RBM-Z, this result also indicates a similar wave-particle interaction occurred in such a wide spatial area, although the latitudinal difference of a few degrees between the ISS and the Arase footprint could be significant, considering a typical scale size of chorus regions (e.g., Shumko et al., 2020).

4.3 Electrostatic whistler event on October 26, 2017

The REP event on October 26, 2017 was identified at geomagnetically active time during a main phase of a moderate magnetic storm. The SYM-H index was at ~-40 nT, AE index of ~900 nT, and the Kp index was 4-. Again, the solar wind speed was high at 530 km/s, as originated from an equatorial coronal hole, and the north-south component of the interplanetary magnetic field in the GSM coordinate system was stable at -4.5 nT since ~1200 UT, which caused the main phase of this magnetic storm.

Electrostatic whistler mode waves were clearly identified as the possible origin of the REP event, as indicated by arrows in Figure 6, at pre-midnight sector of ~20 MLT. The Arase satellite was located around the magnetic equator of 5.5 MLAT, and did not observe EMIC waves (not shown). The ISS passed across the REP region of 61-62 CGMLAT from low to high latitude in the southern hemisphere within 1 min from 1350 UT at 20.5 MLT. The energy spectra

of the energetic electrons were broadband, and the possible energy dispersion from high (~5 MeV) to low (~0.3 MeV) energy was identified by three different instruments of CHD, RBM, and SDOM, although the time resolution of SDOM is not fine enough to resolve it. It is also noteworthy that this event occurred at duskside associated with a relatively complex plasmaspheric boundary (not shown), which may contribute to cause a broad-band resonant energy of electrons associated with the electrostatic whistler waves.

CHD observed an isolated packet of quasi-periodic ~0.2 Hz oscillation of the count rate for the time interval from 1350:00 UT to 1350:30 UT, while similar periodic oscillation was also found in the integrated amplitude of whistler-mode waves at close timing of 1350:10-1350:40 UT. The energy dispersion of this REP event as shown in top three panels of Figure 6 likely reflects the time-of-flight effects of precipitating electrons, i.e., different energy electrons precipitate into the atmosphere from the different latitudes where the pitch angle scattering takes place (Saito et al.. 2012, Miyoshi et al., 2015a, 2015b).

It is noted that a similar ~0.2 Hz oscillation in the intensity of electrostatic waves can be seen earlier at 1348 UT. The signal almost disappeared at the Arase satellite when the closest conjunction was likely achieved with the ISS at 1349 UT, and the ISS did not observe the REP event. When the REP event was observed at 1350 UT, the ISS went away from the Arase footprint, ~2 degrees higher CGMLAT and ~1 MLT later. It is therefore hard to directly compare the REP event and the wave activity in detail. Nevertheless, we can find similar intensity variations in the MeV electron flux and the wave intensities at the close timing of only 10 s difference, as shown by the arrows in Figure 6.

5 Discussions

Let us briefly summarize the obtained results from three different types of REP events. For EMIC event on August 21 (Figures 3 and 4), quasi-periodic signature at ~1 Hz was clearly identified in the CHD count rate at 1735 UT (Figure 2a). This is consistent with the report that similar 1-Hz rapid modulation of isolated proton aurora was induced by Pc1 geomagnetic waves (Ozaki et al., 2018b). On the other hand, the CHD count rate rapidly and irregularly changed (Figure 2b) during the chorus event on April 24 (Figure 5). Electrostatic whistler event on October 26 (Figure 6) did not show such rapid changes, and the profile is rather smooth (Figure 2c). These high temporal resolution data of CHD count rate as shown in Figure 2 can therefore be useful to distinguish the different plasma waves causing the REP events.

Pre-midnight REP events had sometimes been simply interpreted to be associated with EMIC waves (e.g., Kataoka et al., 2016). This study provided such an example showing the essential role of EMIC waves near the magnetic equator (Figures 3 and 4). However, this study also clearly demonstrated that whistler mode chorus waves (Figure 5) and even electrostatic whistler mode waves (Figure 6) can be the major scattering source near the magnetic equator.

It is also noteworthy that the three examples shown above are not likely unique, but similar types of REP events were also identified. For example, similar activity to April 24 event was identified on April 25 (Supplemental Information S1), while similar activity to October 26 event was identified on October 28 (Supplemental Information S2). The clustering occurrence spanning a few days implies that the similar activity can be found, depending on the ISS orbit crossing across similar MLT-CGMLAT regions.

Future works should therefore include a statistical survey to evaluate the relative importance of the whistler mode waves and EMIC waves to cause the REP events during the declining phase of the solar cycle 24, and to evaluate the possible impact of these different plasma waves on the trapped electrons. Open data of the CALET/CHD, MAXI/RBM, and SEDA-AP/SDOM and the Arase satellite will enhance the opportunities of such statistical studies. Identified time profiles of high time cadence CHD data as well as the comparison with RBM count rate will also help to distinguish the plasma waves causing the REP events.

All three events introduced in this study occurred during high-speed solar wind from coronal holes, which encourage us to realize a space weather forecast, based on some future statistical results. However, a caveat should be reminded that the EMIC event occurred during geomagnetically quiet time as was the case of August 21 event, which may be hard to be predicted based on the possible solar wind parameter dependence.

6 Conclusions

Relativistic electrons are scattered and precipitated onto the ISS by various types of plasma waves in the inner magnetosphere. From the conjunction events with the Arase satellite at pre-midnight sector, we identified EMIC waves, chorus waves, and electrostatic whistler mode waves as the different causes of the REP events, during different phases of storms and substorms.

Acknowledgments, Samples, and Data

The CALET/CHD data used in this analysis were provided by the Waseda CALET Operation Center at Waseda University. The MAXI/RBM data used in this study were provided by RIKEN, JAXA, and the MAXI team, which is available via DARTS at JAXA. The CALET/CHD data (http://darts.isas.jaxa.jp/pub/calet/cal-v1.0/CHD/level1.1/) and MAXI/RBM data (http://darts.isas.jaxa.jp/pub/maxi/rbm/) were provided at DARTS website. The SEDA-AP/SDOM data (http://seesproxy.tksc.jaxa.jp/fw/dfw/SEES/English/Top/top_e.shtml) were provided at SEES website. We used the UDAS egg developed by the Inter-university Upper atmosphere Global Observation NETwork (IUGONET) project (http://www.iugonet.org/) to read CALET/CHD data and MAXI/RBM data. Science data of the ERG (Arase) satellite were obtained from the ERG Science Center operated by ISAS/JAXA and ISEE/Nagoya University (https://ergsc.isee.nagoya-u.ac.jp/index.shtml.en). PWE/OFA L2 v02, PWE/EFD L1 prime 2 v01, MGF L2 v03, and OBT L2 v0 are used in this study. RK is supported by JSPS KAKENHI 15H05815, 16H06286, 17K05671. RK and YA are supported by JSPS KAKENHI 17H02901. YM is supported by JSPS KAKENHI 15H05815, 15H05747, 16H06286, 17H00728, 20H01959.

References

Anderson, H. R., Hudson, P. D., and McCoy, J. E. (1968), Observations of POGO ion chamber experiment in the outer radiation zone, J. Geophys. Res., 73, 6285-6297.

Angelopoulos et al. (2019), The Space Physics Environment Data Analysis System (SPEDAS), Space Sci. Rev., 215, 1, 9, 10.1007/s11214-018-0576-4.

Asaoka, Y., Ozawa, S., Torii, S. et al. (CALET collaboration) (2018), On-orbit operations and offline data processing of CALET onboard the ISS. Astroparticle Physics, 100, 29-37.

Bailey, D. K., and Pomerantz, M. A. (1965), Relativistic electron precipitation into the mesosphere at subauroral latitudes, J. Geophys. Res., 70, 5823-5830.

Blake, J. B., M. D. Looper, D. N. Baker, R. Nakamura, B. Klecker, and D. Hovestadt (1996), New high temporal and spatial resolution measurements by SAMPEX of the precipitation of relativistic electrons, Adv. Space Res., 18(8), 171-186.

Carson, B. R., C. J. Rodger, and M. A. Clilverd (2013), POES satellite observations of EMIC-wave driven relativistic electron precipitation during 1998-2010, J. Geophys. Res. Space Physics,118, 232-243, doi:10.1029/2012JA017998.

Comess, M. D., D. M. Smith, R. S. Selesnick, R. M. Millan, and J. G. Sample (2013), Duskside relativistic electron precipitation as measured by SAMPEX: A statistical survey, J. Geophys. Res. Space Physics, 118, 5050?5058, doi:10.1002/jgra.50481.

Daae, M., Espy, P., H. Nesse Tyssoy, Newnham, D., Stadsnes, J. & Soraas, F. (2012), The effect of energetic electron precipitation on middle mesospheric night-time ozone during and after a moderate geomagnetic storm. Geophysical Research Letters, 39, L21811, http://doi.org/doi:10.1029/2012GL053787.

Denton, R. E., Ofman, L., Shprits, Y. Y., Bortnik, J., Millan, R. M., Rodger, C. J., et al. (2019). Pitch angle scattering of sub‐MeV relativistic electrons by electromagnetic ion cyclotron waves. Journal of Geophysical Research: Space Physics, 124, 5610-5626. https://doi.org/10.1029/2018JA026384.

Imhof, W. L., Voss, H. D., Reagan, J. B., Datlowe, D. W., Gaines, E. E., Mobilia, J., and Evans, D. S. (1986), Relativistic electron and energetic ion precipitation spikes near the plasmapause, J. Geophys. Res., 91, 3077-3088.

Isono, Y., Mizuno, A., Nagahama, T., Miyoshi, Y., Nakamura, T., Kataoka, R., Tsutsumi, M., Ejiri, K., Fujiwara, H., Maezawa, H. & Uemura, M. (2014), Ground-based observations of nitric oxide in the mesosphere and lower thermosphere over Antarctica in 2012-2013, J. Geophys. Res.: Space Physics, 119(9), 7745.

Isono, Y., Mizuno, A., Nagahama, T., Miyoshi, Y., Nakamura, T., Kataoka, R., Tsutsumi, M., Ejiri, K., Fujiwara, H., & Maezawa, H. (2014), Variations of nitric oxide in the mesosphere and lower thermosphere over Antarctica associated with a magnetic storm in April 2012, Geophysical Research Letters, 41(7), 2568.

Kasahara, Y., Kasaba, Y., Kojima, H. et al. The Plasma Wave Experiment (PWE) on board the Arase (ERG) satellite. Earth Planets Space 70, 86 (2018) doi:10.1186/s40623-018-0842-4.

Kasaba, Y., Ishisaka, K., Kasahara, Y. et al. Wire Probe Antenna (WPT) and Electric Field Detector (EFD) of Plasma Wave Experiment (PWE) aboard the Arase satellite: specifications and initial evaluation results. Earth Planets Space 69, 174 (2017) doi:10.1186/s40623-017-0760-x

Kataoka, R., Asaoka, Y., Torii, S., Terasawa, T., Ozawa, S., Tamura, T., Shimizu, Y., Akaike, Y., & Mori, M. (2016), Relativistic electron precipitation at International Space Station: Space weather monitoring by Calorimetric Electron Telescope. Geophysical Research Letters, 43, 4119-4125, http://doi.org/doi:10.1002/2016GL068930.

Kataoka, R., Nishiyama, T., Tanaka, Y. et al. Transient ionization of the mesosphere during auroral breakup: Arase satellite and ground-based conjugate observations at Syowa Station. Earth Planets Space 71, 9 (2019). https://doi.org/10.1186/s40623-019-0989-7.

Kubota, Y., Omura, Y., and Summers, D. (2015), Relativistic electron precipitation induced by EMIC-triggered emissions in a dipole magnetosphere, J. Geophys. Res. Space Physics, 120, 4384, 4399, doi:10.1002/2015JA021017.

Kurita, S., Miyoshi, Y., Shiokawa, K., Higashio, N., Mitani, T., Takashima, T., et al. (2018). Rapid loss of relativistic electrons by EMIC waves in the outer radiation belt observed by Arase, Van Allen Probes, and the PWING ground stations, Geophysical Research Letters, 45, 12,720-12,729. https://doi.org/10.1029/2018GL080262.

Lorentzen, K. R., McCarthy, M. P., Parks, G. K., Foat, J. E., Millan, R. M., Smith, D. M., Lin, R. P. & Treilhou J. P. (2000), Precipitation of relativistic electrons by interaction with electromagnetic ion cyclotron waves, Geophysical Research Letters, 105, 5381-5389.

Matsumoto, H., Koshiishi, H., Goka, T., Kimoto, Y., Green, B. D., Galica, G. E., Nakamura, T., Abe, T., Badono, S., Murata, S., & Sullivan, J. D. (2001), Compact, lightweight spectrometer for energetic particles, IEEE Transactions on Nuclear Science, 48(6), 2043-2049.

Matsuoka, M., et al. (2009), The MAXI mission on the ISS: Science and instruments for monitoring All-sky X-ray Images, Publications of the Astronomical Society of Japan, 61(5), 999-1010.

Matsuoka, A., Teramoto, M., Nomura, R. et al. The ARASE (ERG) magnetic field investigation. Earth Planets Space 70, 43 (2018) doi:10.1186/s40623-018-0800-1.

McIlwain, C. E. (1961), Coordinates for mapping the distribution of magnetically trapped particles, J. Geophys. Res., 66(11), 3681? 3691, doi:10.1029/JZ066i011p03681.

Millan, R. M., R. P. Lin, D. M. Smith, K. R. Lorentzen (2002), and M. P. McCarthy, X-ray observations of MeV electron precipitation with a balloon-borne germanium spectrometer, Geophys. Res. Lett., 29(24), 2194, doi: 10.1029/2002GL015922.

Millan, R. M, and R. M. Thorne (2007), Review of radiation belt relativistic electron losses, J. Atm. Solar-Terr. Phys., 69, 362.Miyoshi, Y., K. Sakaguchi, K. Shiokawa, D. Evans, J. Albert, M. Conners, and V. Jordanova (2008), Precipitation of radiation belt electrons by EMIC waves, observed from ground and space, Geophys. Res. Lett., 35, L23101, doi:10.1029/2008GL035727.

Miyoshi, Y., Sakaguchi, K., Shiokawa, K., Evans, D., Albert, J., Connors, M., and Jordanova, V. (2008), Precipitation of radiation belt electrons by EMIC waves, observed from ground and space, Geophys. Res. Lett., 35, L23101, doi:10.1029/2008GL035727.

Miyoshi, Y., S. Oyama, S. Saito, H. Fujiwara, R. Kataoka, Y. Ebihara, C. Kletzing, G. Reeves, O. Santolik, M. Cliverd, C. Rodger, E. Turunen, and F. Tsuchiya (2015a), Energetic electron precipitation associated with pulsating aurora: EISCAT and Van Allen Probes observations, J. Geophys. Res., 120, doi:10.1002/2014JA020690.

Miyoshi, Y., et al. (2015b), Relation between fine structure of energy spectra for pulsating aurora electrons and frequency spectra of whistler mode chorus waves, J. Geophys. Res. Space Physics, 120, doi:10.1002/2015JA021562.

Miyoshi, Y., I. Shinohara,, T. Takashima, K. Asamura, N. Higashio, T. Mitani, S. Kasahara, S. Yokota, Y. Kazama, S.-Y. Wang, S. W. Tam, P. T. P Ho, Y. Kasahara, Y. Kasaba, S. Yagitani, A. Matsuoka, H. Kojima, H. Katoh, K. Shiokawa, and K. Seki (2018a), Geospace Exploration Project ERG, Earth, Planets and Space, 10.1186/s40623-018-0862-0.

Miyoshi, Y., T. Hori, M. Shoji, M. Teramoto, T. F. Chang, S. Matsuda, S. Kurita, T. Segawa, N. Umemura, K. Keika, Y. Miyashita, Y. Tanaka, N. Nishitani, T. Takashima, and I. Shinohara (2018b), The ERG Science Center, Earth, Planets and Space, 10.1186/s40623-018-0867-8.

Nakamura, R., D. N. Bake, J. B. Blake, S. Kanekal, B. Klecker, and D. Hovesta (1995), Relativistic electron precipitation enhancements near the outer edge of the radiation belt, Geophys. Res. Lett., 22, 1129?1132, doi:10.1029/95GL00378.

Nakamura, R., M. Isowa, Y. Kamide, D. N. Baker, J. B. Blake, and M. Looper (2000), SAMPEX observations of precipitation bursts in the outer radiation belt, J. Geophys. Res., 105(A7), 15875-15885, doi:10.1029/2000JA900018.

Ozaki, M., Yagitani, S., Kasahara, Y. et al. (2018a) Magnetic Search Coil (MSC) of Plasma Wave Experiment (PWE) aboard the Arase (ERG) satellite. Earth Planets Space 70, 76, doi:10.1186/s40623-018-0837-1

Ozaki, M., Shiokawa, K., Miyoshi, Y., Kataoka, R., Connors, M., Inoue, T., … Danskin, D. W. (2018b). Discovery of 1 Hz range modulation of isolated proton aurora at subauroral latitudes. Geophysical Research Letters, 45, 1209-1217. https://doi.org/10.1002/2017GL076486

Rosenberg, T. J., Lanzerotti, L. J., Bailey, D. K., and Pierson, J. D. (1972), Energy spectra in relativistic electron precipitation events, J. Atmos. Terr. Phys., 34, 1977-1989.

Saito, S., Y. Miyoshi, and K. Seki (2012), Relativistic electron microbursts associated with whistler chorus rising tone elements: GEMSIS-RBW simulation, J. Geophys. Res., 117, A10206, doi:10.1029/2012JA018020.

Shumko, M., Johnson, A. T., Sample, J. G., Griffith, B. A., Turner, D. L., O'Brien, T. P., et al. (2020). Electron microburst size distribution derived with AeroCube-6. Journal of Geophysical Research: Space Physics, 125, e2019JA027651. https://doi.org/10.1029/2019JA027651

Shepherd, S. G. (2014), Altitude-adjusted corrected geomagnetic coordinates: Definition and functional approximations, J. Geophys. Res. Space Physics, 119, 1-21, doi:10.1002/2014JA020264.

Tanaka, Y.-M., Nishiyama, T., Kadokura, A., Ozaki, M., Miyoshi, Y., Shiokawa, K., et al. (2019). Direct comparison between magnetospheric plasma waves and polar mesosphere winter echoes in both hemispheres. Journal of Geophysical Research: Space Physics, 124. https://doi.org/10.1029/2019JA026891.

455 Torii, S., et al. (2017), The CALorimetric Electron Telescope (CALET) on the ISS: Preliminary
456 Results from On-orbit Observations since October, 2015, in Proceeding of Science
457 (ICRC2017), 1092.

458 Tsyganenko, N. A., and Sitnov, M. I. (2005), Modeling the dynamics of the inner magnetosphere
459 during strong geomagnetic storms, J. Geophys. Res., 110, A03208,
460 doi:10.1029/2004JA010798.

461 Turunen, E., A. Kero, P. T. Verronen,Y. Miyoshi, S.-I. Oyama, and S. Saito (2016),
462 Mesospheric ozone destruction by high-energy electron precipitation associated with
463 pulsating aurora, J. Geophys. Res. Atmos., 121, doi:10.1002/2016JD025015.

464 Ueno, H., Nakahira, S., Kataoka, R., Asaoka, Y., Torii, S., Ozawa, S., et al (2019). Radiation
465 dose during relativistic electron precipitation events at the International Space Station.
466 Space Weather, 17. https://doi.org/10.1029/2019SW002280.

467

468 **Table 1.** Energy range of electrons as observed by SDOM, CHD, and RBM (after Ueno et al.,
469 2019).

Instruments	Energy range of electrons [MeV]
SEDA-AP/SDOM CH1	0.28-0.79
SEDA-AP/SDOM CH2	0.93-1.85
SEDA-AP/SDOM CH3	1.58-3.44
SEDA-AP/SDOM CH4	3.30-5.50
SEDA-AP/SDOM CH5	5.31-10.23
CALET/CHD X	> 1.6
CALET/CHD Y	> 3.6
MAXI/RBM	> 0.3

470

Figure 1. The ISS or

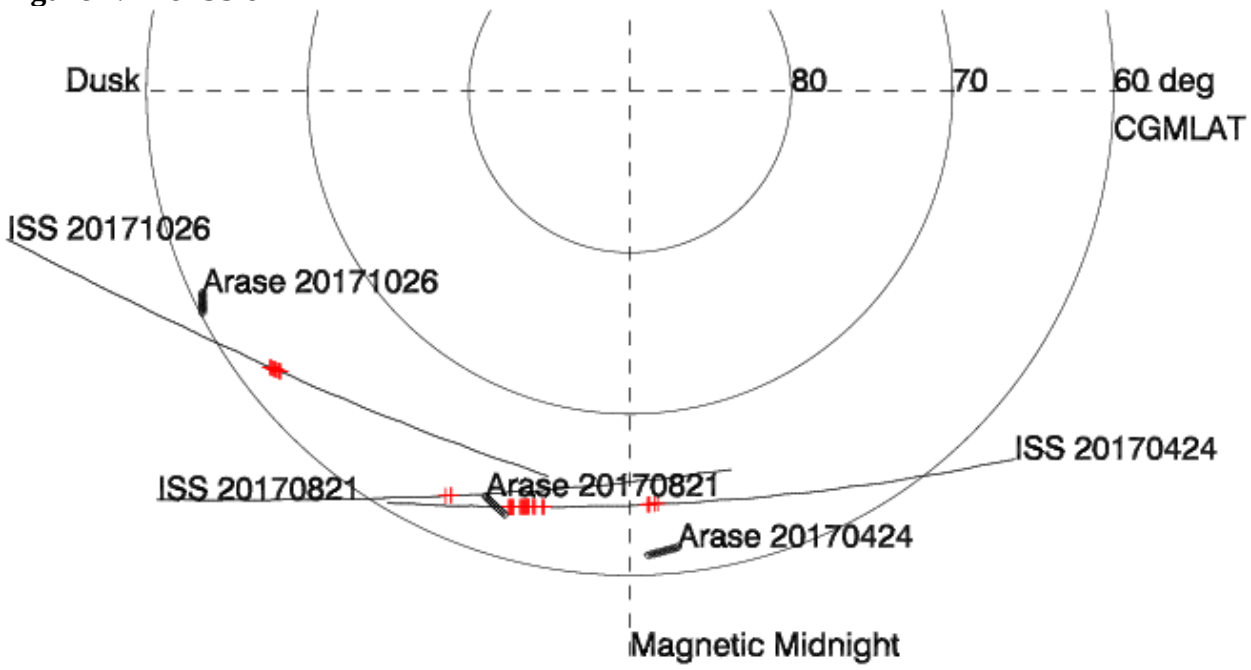

bit (black curves) and the Arase footprint (diamonds) during the 10 min time intervals of three selected REP events. The AACGM coordinate system was used to show the polar map, center is

476 the south pole (CGMLAT = -90 deg), 12 MLT is to the top, and 18 MLT is to the left. The red
477 plus signs indicate the large count rate (>5×10^4 Hz) of CHD-X.

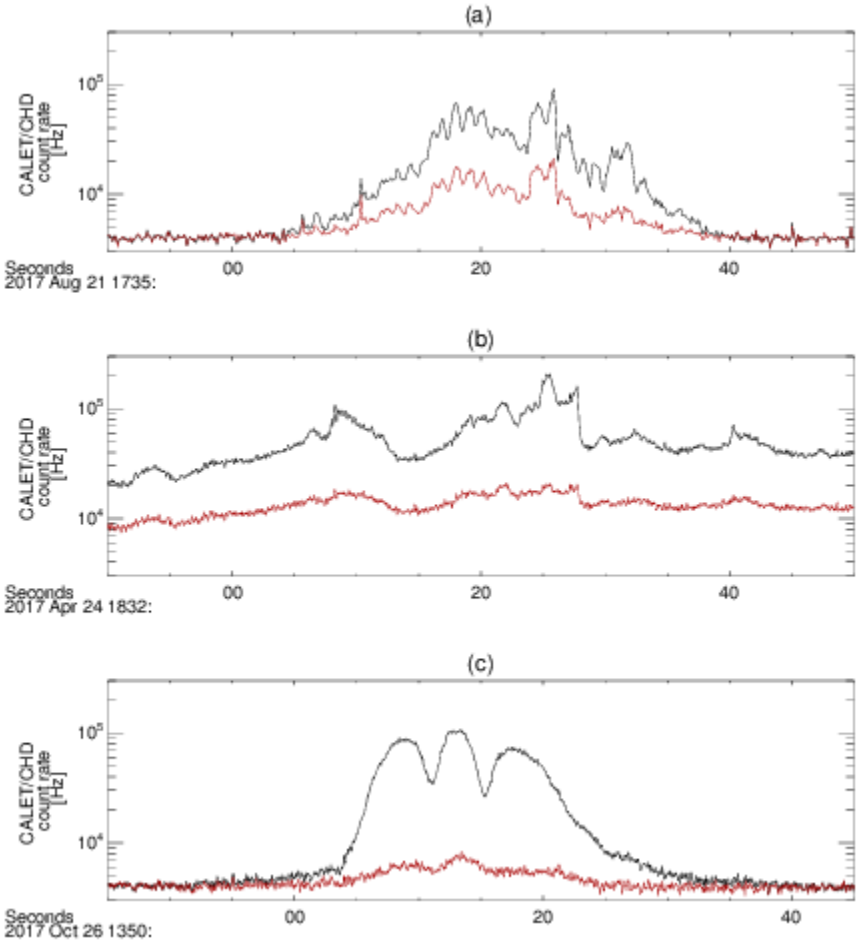

478

479 **Figure 2**. High time cadence count rate data of CHD-X (black) and CHD-Y (red) at 0.1 s time
480 cadence; (top) quasi-periodic variation associated with EMIC waves, (middle) irregular variation

associated with chorus waves, and (bottom) smooth and quasi-periodic variation associated with electrostatic whistler waves.

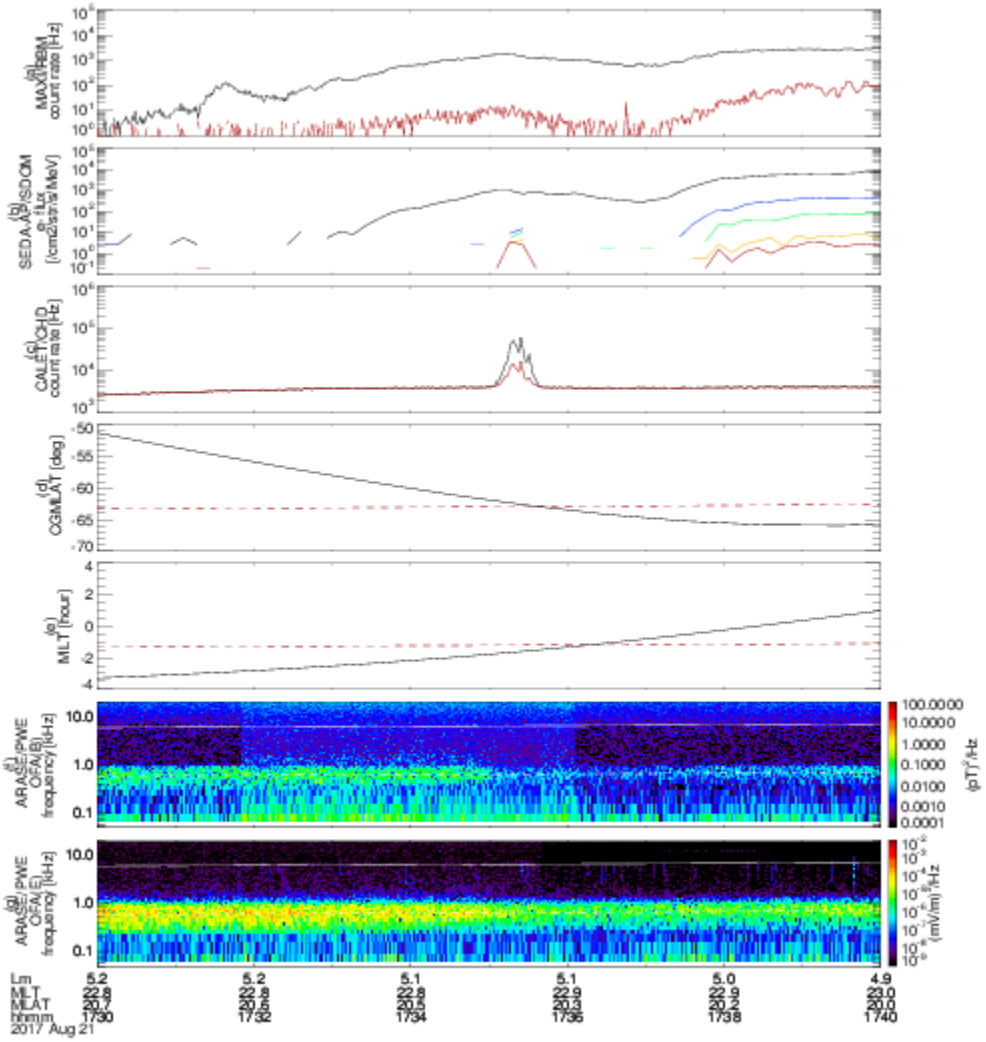

Figure 3. The REP event on August 21, 2017. From top to bottom, (a) MAXI/RBM count rate (red: RBM-Z, black: RBM-H), (b) SEDA-AP/SDOM electron flux CH1-5, (c) CALET/CHD count rate (red: CHD-Y, black: CHD-X), (d) magnetic latitudes of the ISS (black) and of the Arase footprint (red dashed), (e) magnetic local time of the ISS (black curve) and of the Arase footprint (red dashed curve), (f) OFA magnetic field spectra with fce and 0.1 fce at magnetic equator (white curve and dashed white curve), and (g) OFA electric field spectra. The fce was calculated via the magnetic field tracing using the IGRF model. Note that Lm is McIlwain's *L*

value (McIlwain, 1961) and the magnetic latitude (MLAT) were also derived from the IGRF model.

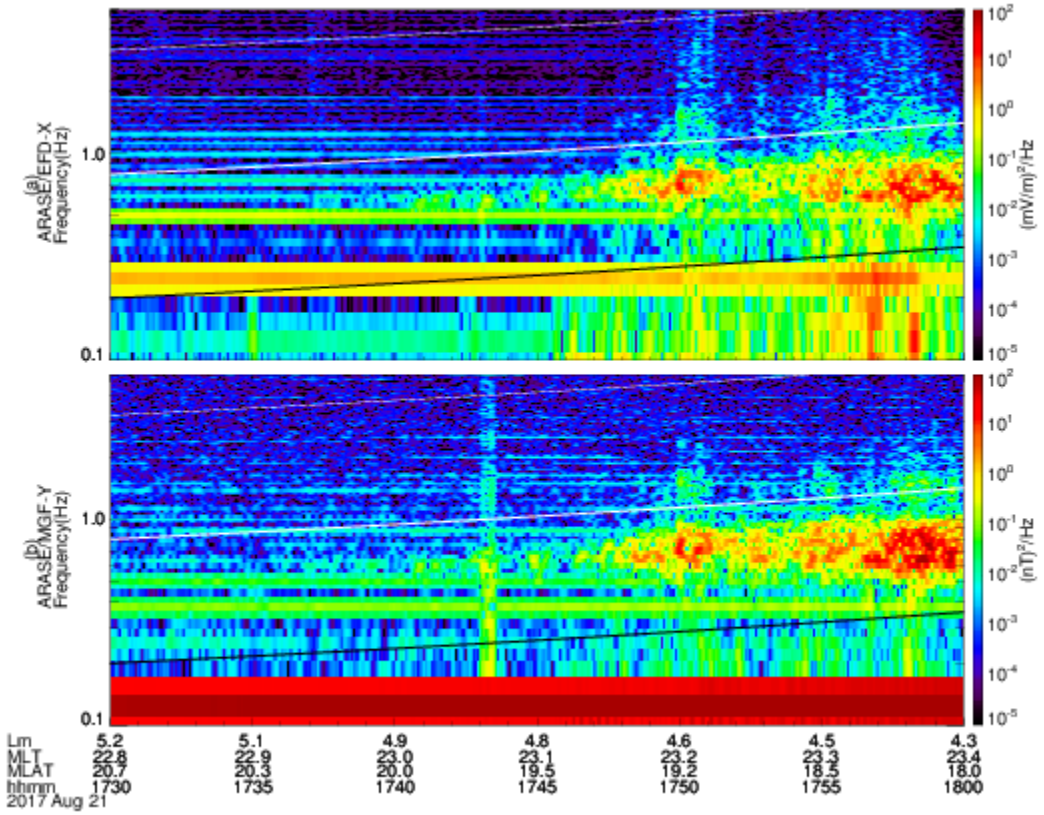

Figure 4. Dynamic spectrum of the (top) EFD-X and (bottom) MGF-Y of the Arase satellite. Cyclotron frequency of He+ and O+ at magnetic equator are shown by white and black curves, respectively. He+ band EMIC waves from 0.5-1.0 Hz were clearly detected after 1740 UT.

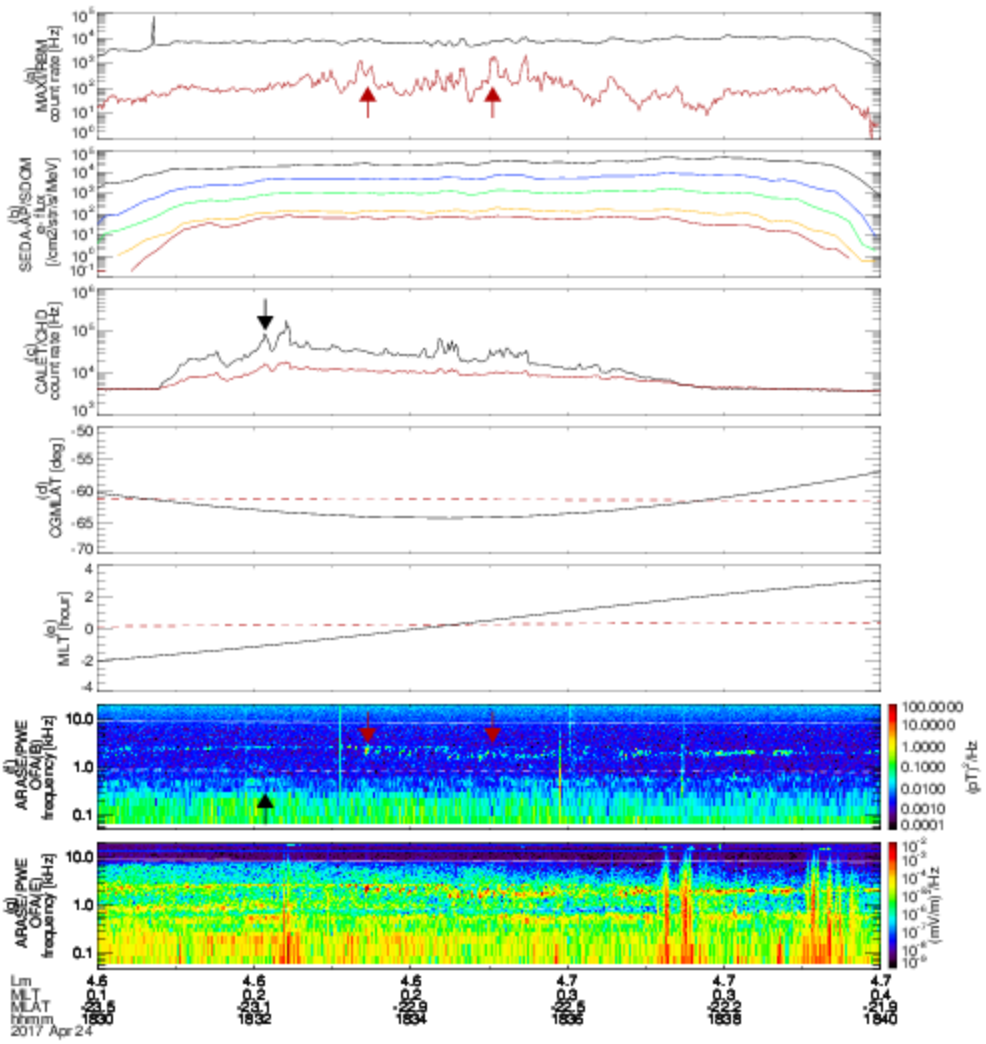

Figure 5. The REP event on April 24, 2017. Format is the same as Figure 3. Arrows indicate the possible correlations between the count rate increases and plasma wave intensifications.

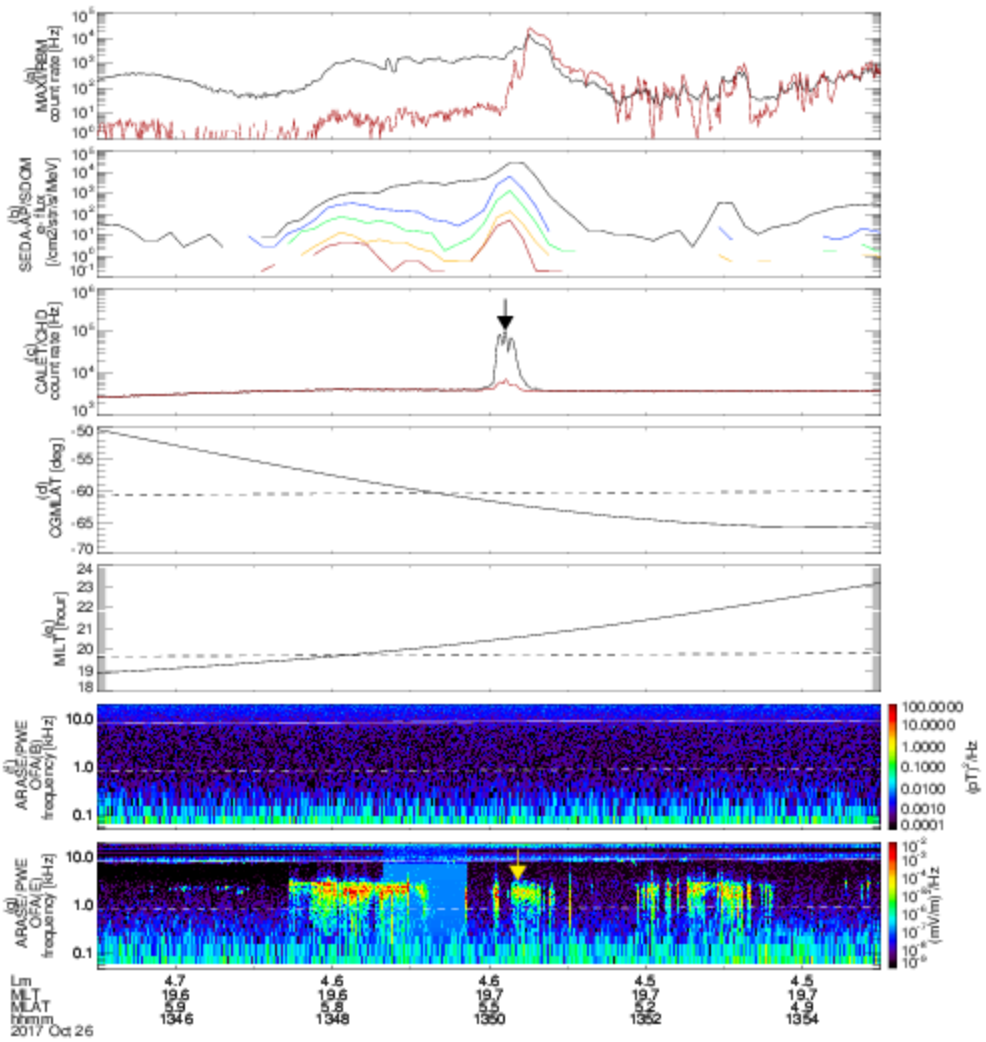

Figure 6. The REP event on October 26, 2017. Format is the same as Figure3. Arrows indicate the possible correlations between the count rate increases and plasma wave intensifications.